Taylor & Francis
Taylor & Francis Group

Neurological Research

A Journal of Progress in Neurosurgery, Neurology and Neurosciences

ISSN: 0161-6412 (Print) 1743-1328 (Online) Journal homepage: www.tandfonline.com/journals/yner20

Identification of autophagy-related biomarkers in the circulatory system of ischemic stroke

Yuyu Xu, Jinshan Duan, Deling Zhong, Ming Yuan, Guohai Zhang, Zheli Zhu & Yani Xie

To cite this article: Yuyu Xu, Jinshan Duan, Deling Zhong, Ming Yuan, Guohai Zhang, Zheli Zhu & Yani Xie (02 Sep 2025): Identification of autophagy-related biomarkers in the circulatory system of ischemic stroke, Neurological Research, DOI: 10.1080/01616412.2025.2556537

To link to this article: https://doi.org/10.1080/01616412.2025.2556537

NEUROLOGICAL RESEARCH
https://doi.org/10.1080/01616412.2025.2556537

Taylor & Francis
Taylor & Francis Group

Identification of autophagy-related biomarkers in the circulatory system of ischemic stroke

Yuyu Xu[a], Jinshan Duan[a], Deling Zhong[a], Ming Yuan[a], Guohai Zhang[b], Zheli Zhu[a] and Yani Xie[a]

[a]Department of Neurology, The Shengzhou Hospital of Traditional Chinese Medicine, Shengzhou, Zhejiang Province, China; [b]Department of Neurosurgery, The Shengzhou Hospital of Traditional Chinese Medicine, Shengzhou, Zhejiang Province, China

ABSTRACT

Objectives: Increasing evidence indicates autophagy's dual role in ischemic stroke (IS), though its mechanisms and biomarkers remain unclear. This study analyzes autophagy-related genes (ARGs) and constructs a circRNA-miRNA-mRNA network to identify key ARGs and their interactions.

Materials and Methods: Differentially expressed genes from GEO were intersected with HADb-derived autophagy-related genes (ARGs) to identify DEARGs. Target mRNAs of DEmiRNAs and DEcircRNAs were predicted via mirDIP and circBank, respectively, and integrated to construct a circRNA-miRNA-mRNA regulatory network. Key genes were screened through PPI analysis, followed by immune infiltration analysis and experimental validation.

Results: In IS, 539 circRNAs, 61 miRNAs, and 565 mRNAs were identified with differential expression. A circRNA-miRNA-autophagy related mRNA network was established, identifying multiple regulatory relationship pairs. Notably, five autophagy-related hub genes demonstrated significant correlations with immune cell infiltration. Clinical validation further confirmed that (HIF1A) and (EIF2AK2) were significantly upregulated, while (HSPA8) was significantly downregulated, underscoring their potential relevance in IS.

Conclusion: HIF1A, EIF2AK2, and HSPA8 May serve as biomarkers for early diagnosis of IS. This study reveals fresh insights into the molecular mechanisms linked to IS.

ARTICLE HISTORY
Received 16 June 2025
Accepted 29 August 2025

KEYWORDS
Ischemic stroke; autophagy; biomarker; circRNA-miRNA-autophagy related mRNA network; immune cell

Introduction

Stroke refers to the disruption or reduction of blood supply to the brain, leading to inadequate oxygen and nutrients to brain tissues [1]. Worldwide, it is still the second top cause of death and the third top cause of disability. Stroke reduces the quality of life for patients and adds a significant economic strain on society, with global medical costs associated with stroke exceeding 721 billion dollars [2]. Globally, about 87% of strokes are ischemic strokes (IS), while hemorrhagic strokes account for a smaller percentage [2]. The main clinical symptoms of IS include speech impairments, consciousness disturbances, facial drooping, hemiplegia, loss of coordination, and balance disorders, which can even be life-threatening [3,4]. Early recognition of IS can significantly reduce the risk of stroke and improve prognosis [5]. Although the treatment options for IS, such as intravenous thrombolysis and mechanical thrombectomy, have rapidly advanced, the treatment outcomes remain limited due to the inability to administer timely interventions [6]. However, the risk factors of IS are complex and diverse, and there is still a lack of effective methods for accurately predicting IS, making the search for predictive and diagnostic biomarkers an urgent and clinically significant task [7,8].

Accumulating evidence underscores the pivotal yet paradoxical role of autophagy in IS pathogenesis. Physiological levels of autophagy, induced by mild ischemic stress, serve as a cytoprotective mechanism to maintain cellular homeostasis by clearing damaged organelles and misfolded proteins. Conversely, prolonged or severe ischemia triggers aberrant hyperactivation of autophagy, resulting in excessive degradation of essential cellular components and ultimately contributing to neuronal death, thereby positioning autophagy as a double-edged sword in IS [9]. Given its dual role, therapeutic modulation of autophagy – either by enhancing protective autophagy during early ischemia or suppressing detrimental hyperactivation

CONTACT Yuyu Xu dr_xuyuyu@163.com Department of Neurology, The Shengzhou Hospital of Traditional Chinese Medicine, 208 Yiyuan Road, Shengzhou, Zhejiang Province 312400, China

in prolonged injury – represents a promising strategy for IS intervention. Despite prior efforts to identify autophagy-associated biomarkers (e.g. LC3, Beclin-1, and Cyto-ID) for IS diagnosis, these candidates remain limited by inadequate clinical validation and lack of specificity [10,11].

In addition to coding RNAs, non-coding RNAs like microRNA (miRNA) and circular RNA (circRNA) are also play crucial roles in IS. MiRNAs, typically around 22 nucleotides in length, modulate gene expression by binding to the 3' untranslated regions (UTRs) of target messenger RNAs (mRNAs), thereby inhibiting translation or promoting mRNA degradation [12]. CircRNAs, a newly discovered class of endogenous non-coding RNAs characterized by their closed-loop structures, function as molecular sponges for miRNAs, thereby regulating miRNA activity and influencing processes such as protein coding and the expression of other genes [13]. It is estimated that more than 2,000 identified miRNAs may regulate approximately one-third of human genes [14]. Research aimed at identifying biomarkers associated with IS has uncovered numerous miRNAs and circRNAs with aberrant expression patterns, including miR-125-5p, miR-4446-3p, circ-PTP4A2, and circ-TLK2. These molecules are implicated in various biological processes such as autophagy, apoptosis, immunity, and inflammation [15–18]. Consequently, miRNAs and circRNAs hold promise as potential predictive biomarkers and therapeutic targets for IS.

IS triggers a cascade of neuroinflammatory responses through multiple cellular and molecular mechanisms. Injured cells upregulate selectins, promoting leukocyte adhesion to the vascular endothelium while compromising blood-brain barrier (BBB) integrity. This barrier disruption facilitates the extravasation of danger-associated molecular patterns (DAMPs) into both systemic circulation and cerebrospinal fluid, subsequently activating innate immune responses through sequential signaling pathways [19]. A spectrum of immune cells, including microglia, monocytes, neutrophils, astrocytes, T lymphocytes, and B lymphocytes, have been demonstrated to participate extensively in post-IS neuroinflammation [20,21]. The inflammatory mediators (cytokines and chemokines) released by these immune cells not only mediate local inflammatory responses but also disseminate systemically via circulation, forming an 'invisible regulatory network' that connects central nervous system (CNS) pathology with peripheral immune status. Nevertheless, the precise relationships between blood-based biomarkers of IS and specific immune cell subsets remain to be fully elucidated, representing a critical knowledge gap in understanding the holistic immunopathological mechanisms of IS.

This study aims to identify key autophagy-related genes (ARGs) involved in IS and the potential circRNA-miRNA-autophagy related mRNA network relationships. To achieve this, we leveraged publicly available datasets from the Gene Expression Omnibus (GEO) database to identify differentially expressed mRNAs, miRNAs, and circRNAs in the context of IS. Subsequently, we constructed a comprehensive circRNA-miRNA-autophagy related mRNA network. Through rigorous protein-protein interaction (PPI) analysis, we identified the key genes in this network and analyzed their relationships with immune cells. Finally, we substantiated the differential expression of these hub genes by validating them against the public dataset GSE58294 and blood samples from a clinical cohort, employing quantitative real-time polymerase chain reaction (qRT-PCR) and Western blot techniques.

Methods

Data collection

We searched the the public datasets using 'ischemic stroke' in the GEO database and identified four datasets, each of which characterized different aspects of gene expression related to IS: Whole blood mRNA expression data, GSE16561 (GPL6883 Illumina HumanRef-8 v3.0 expression beadchip), which includes samples from 24 healthy controls (HC) and 39 IS patients. Whole blood mRNA expression data at various time points post-IS, GSE58294 (GPL570 Affymetrix Human Genome U133 Plus 2.0 Array), comprising 23 HC and 23 IS patients, with samples collected 3 h, 5 h, and 24 h after stroke onset. Plasma circRNA expression data, GSE133768 (GPL21825 074301 Arraystar Human CircRNA microarray V2), featuring 3 HC and 3 IS. Plasma miRNA expression data, GSE199942 (GPL16791 Illumina HiSeq 2500 Homo sapiens), including 5 HC and 5 IS patients. Additionally, we obtained a list of 222 ARGs from the Human Autophagy Database (http://www.autophagy.lu/). Figure 1 shows the data analysis process.

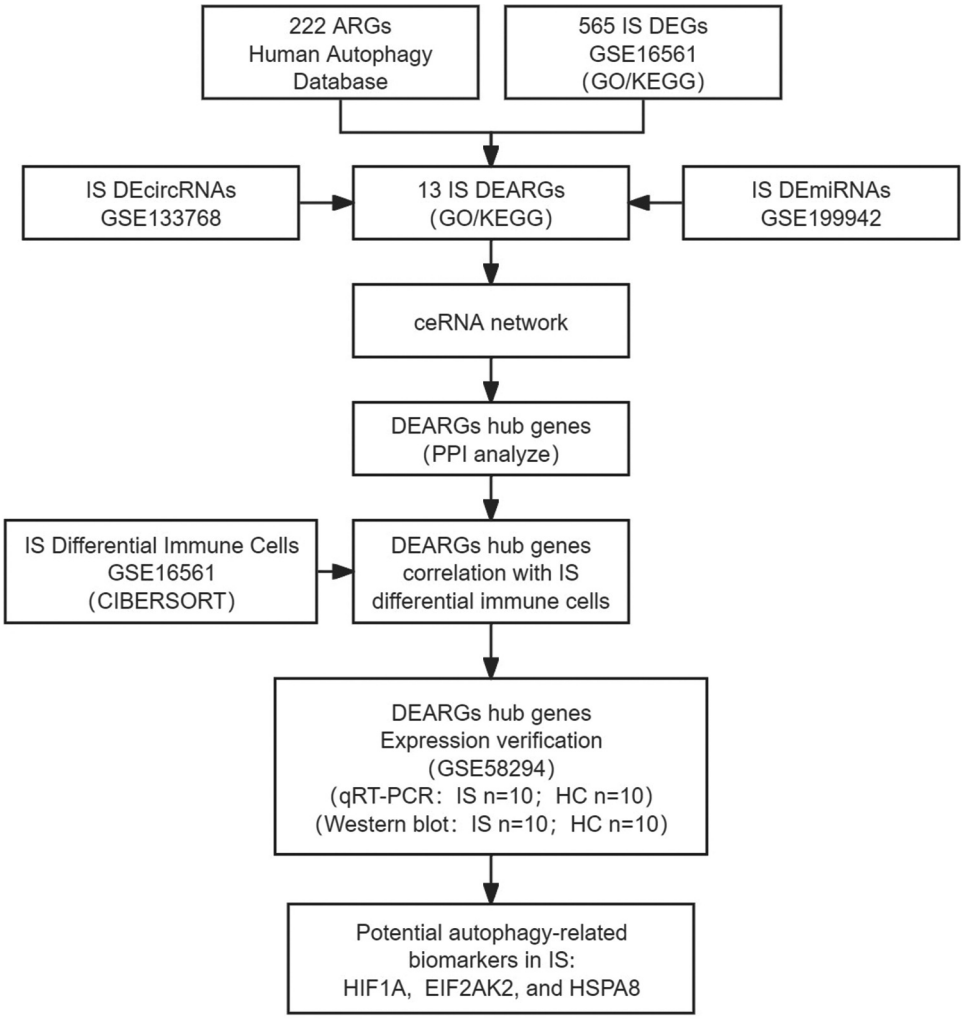

Figure 1. Research workflow diagram. ARGs: Autophagy-related genes, IS: Ischemic stroke, DEGs: Differentially expressed genes, DEcircRNAs: Differentially expressed circRNAs, DEARGs: Differentially expressed autophagy-related genes, DEmiRNAs: Differentially expressed miRNAs, ceRNA: Competing endogenous RNA networks, PPI: Protein-protein interactions.

Identification of differentially expressed mRNA, miRNA, and circRNA

To preprocess the four datasets and remove batch effects, we utilized the 'sva' package (version 3.35.2) in R (version 4.3.0), applying it individually to each dataset. For the mRNA (GSE16561) and miRNA (GSE199942) datasets obtained from RNA-seq, we employed the 'edgeR' package (version 3.42.4) to analyze the differential expression of genes and miRNAs in IS compared to HC. We set the threshold for differentially expressed genes (DEGs) and miRNAs (DEmiRNAs) as $p < 0.05$ and $|\log_2$ fold change $(\log_2 FC)| > 0.5$ [22–24]. For the circRNA dataset (GSE133768), which was acquired via microarray technology, we conducted differential expression analysis using the 'limma' package (version 3.56.2). We defined the criteria for differentially expressed circRNAs (DEcircRNAs) in ischemic stroke, using HC as the reference group, with $p < 0.05$ and $|\log 2FC| > 1$ [16,23].

Identification and functional enrichment analysis of differentially expressed ARGs in IS

To identify ARGs that are differentially expressed in IS, we intersected the list of DEGs with the list of ARGs obtained from the Human Autophagy Database. A set of differentially expressed ARGs (DEARGs) in IS was obtained from this intersection.

To explore the potential biological roles of these DEARGs, we conducted enrichment analysis for Gene Ontology (GO) terms and Kyoto Encyclopedia of Genes and Genomes (KEGG) pathway using the 'clusterProfiler' package (version 4.8.3) in R. Statistical significance for gene enrichment was considered

at $p < 0.05$. This analysis aims to identify the biological processes (BP), cellular components (CC), and molecular functions (MF) as well as the metabolic and signaling pathways that are significantly associated with the DEARGs in the context of IS.

Construction of circRNA-miRNA-autophagy-related mRNA network in IS

The target mRNA of DEmiRNA was predicted through the mirDIP database (https://ophid.utoronto.ca/mirDIP). We then compared the target mRNAs of these predictions with DEARGs and combined expression values to identify relationships in which DEmiRNAs may exert negative regulation on DEARGs. Additionally, using the circBank database (http://www.circbank.cn/), we predicted the target circRNAs for the DEmiRNAs and intersected these predictions with the DEcircRNAs identified in our dataset. Similarly, negatively regulated DEcircRNA-DEmiRNA interaction pairs were selected based on expression values. Finally, we integrated the relationships between DEcircRNAs and DEmiRNAs with those between DEmiRNAs and DEARGs to construct a comprehensive circRNA-miRNA-autophagy-related mRNA network. This network visualization was done with Cytoscape (version 3.9.1). This visualization aids in understanding their roles in regulating autophagy-related processes during IS.

Screening of DEARG hub genes in IS

In the STRING database, the DEARGs were uploaded with 'Homo sapiens' selected as the species and an interaction confidence threshold of at least 0.4, while other parameters were kept at their default values. This process yielded PPI information. The data was then exported in TSV format and brought into Cytoscape (version 3.9.1). Within Cytoscape, the cytoHubba plugin was utilized to calculate various centrality metrics for each gene, including Degree, Betweenness Centrality, and Closeness Centrality. Genes exceeding the median values for all three metrics were selected as hub genes.

Correlation analysis between hub genes and blood immune cells

To assess the distribution of immune cell subtypes in IS patients' the blood, we employed the CIBERSORT tool (http://CIBERSORT.stanford.edu/) to analyze the gene expression matrix from GSE16561, which provided the distribution of 22 types of immune cells. The differences in the distribution of immune cell subtypes between IS patients and HC individuals were displayed using box plots. Subsequently, we identified immune cells that showed significant differences between IS patients and HC. Then, we performed Pearson correlation analysis to assess the correlation between immune cell distribution and hub gene expression in IS samples.

Verification of hub gene expression in IS

We analyzed the expression changes of hub genes at 3 h, 5 h, and 24 h after IS occurrence in the GSE58294 dataset and visualized these changes using violin plots.

In addition, the levels of hub gene expression in blood from IS patients and HC were measured using qRT-PCR and Western blot. This project received approval from the ethics committee of Shengzhou Hospital of Traditional Chinese Medicine (Approval NO: SZZYK-2024–002). The inclusion criteria for IS patients included: (1) aged 18–75 years; (2) diagnosed with IS based on head computerized tomography (CT) or magnetic resonance imaging (MRI); (3) no significant neurological impairment caused by cerebral vascular disorders or other causes prior to the onset; and (4) no history of stroke. The exclusion criteria for IS patients included: (1) stroke occurrence more than 72 h prior; (2) presence of malignant tumors, severe pulmonary infection, severe dysfunction of heart, liver, or kidney, or hemorrhagic diseases causing neurological deficits not related to cerebrovascular reasons; (3) cardioembolic stroke, transient ischemic attack, hemorrhagic infarction, occult cerebral vascular malformation, traumatic cerebrovascular disease; and (4) incomplete clinical data. The inclusion criteria for HC included: (1) aged 18–75 years; (2) have no past incidents of stroke or

Table 1. Baseline characteristics analysis of the two groups.

Item		Healthy controls	IS	*P*
Gender (n, %)	female	3 (30%)	3 (30%)	1
	male	7 (70%)	7 (70%)	
Age (SEM±SD)		68.50 ± 6.50	65.80 ± 8.69	0.442
Complicated with hypertension (n, %)		0 (0%)	7 (70%)	0.005**
Complicated with diabetes (n, %)		0 (0%)	2 (20%)	0.456
Complicated with coronary heart disease (n, %)		0 (0%)	0 (0%)	1
Stroke type (n, %)	large artery atherosclerosis	/	6 (60%)	/
	Small vessel occlusion	/	4 (40%)	
Time of stroke onset (h) (SEM±SD)		/	11.10 ± 10.85	/
NIHSS on admission (SEM±SD)		/	4.60 ± 3.89	/

** indicates $p < 0.01$.

other cardiovascular diseases. The exclusion criteria for HC included: (1) severe head trauma in the past or undergone head surgery; (2) pregnancy or lactation.

Based on these criteria, we recruited 10 IS patients and 10 HC from Shengzhou Hospital of Traditional Chinese Medicine and collected their whole blood samples to examine the mRNA expression levels of hub genes [16]. In addition, 10 IS patients and 10 HC were recruited, and their whole blood was collected to separate the buffy coat and detect the protein expression level of hub genes in the buffy coat. Table 1 presents a comparison of the baseline information of the two groups of patients. The informed consent form was signed by all participants and their families after obtaining their consent.

qRT-PCR

Blood samples from HC were collected during their routine health examinations, while blood samples from IS patients were collected upon hospital admission. 2.5 mL whole blood was collected using PAXgene® Blood RNA Tubes (BD Biosciences, U.S.A.). Total RNA was extracted from the whole blood using the EZ-press Whole Blood RNA Purification Kit (EZ Bioscience, U.S.A.). cDNA was synthesized from total RNA using HiScript III RT SuperMix for qPCR (+gDNA wiper) (Vazyme, China). The oligodT and Random primers for reverse transcription cDNA are from Vazyme (item number R323). Quantitative PCR was performed using Taq Pro Universal SYBR qPCR Master Mix (Vazyme, China), following the manufacturer's instructions. The reference gene used was GAPDH. The target genes' relative expression levels were determined using the $2^{-\Delta\Delta Ct}$ method. Information about the primers used is provided in Table 2.

Western blot

Take 5 mL of blood in an EDTA anticoagulant tube and centrifuge at 2000 g for 15 min at room temperature to separate it into plasma, red blood cells, and a buffy coat containing white blood cells. Carefully aspirate the buffy coat for protein detection. The BCA protein assay kit (Beyotime,

Table 2. Primer sequences used in quantitative PCR.

Primer name	Sequence (5′-3′)
homo-GAPDH-F	GCATCCTGGGCTACACTGAG
homo-GAPDH-R	GTCAAAGGTGGAGGAGTGGG
homo-BNIP3L-F	TTGGATGCACAACATGAATCAGG
homo-BNIP3L-R	TCTTCTGACTGAGAGCTATGGTC
homo-EIF2AK2-F	ACGCTTTGGGGCTAATTCTTG
homo-EIF2AK2-R	CCCGTAGGTCTGTGAAAAACTT
homo- HIF1A-F	GAACGTCGAAAAGAAAAGTCTCG
homo- HIF1A-R	CCTTATCAAGATGCGAACTCACA
homo-HSPA8-F	ACTCCAAGCTATGTCGCCTTT
homo-HSPA8-R	TGGCATCAAAAACTGTGTTGGT
homo-LAMP2-F	TGGCAATGATACTTGTCTGCTG
homo-LAMP2-R	ACGGAGCCATTAACCAAATACAT

China) was employed to determine the protein concentration. The protein samples were then diluted with protein loading buffer to a final concentration of 5 mg/mL. A 10 μL aliquot of each protein sample was resolved by sodium dodecyl sulfate-polyacrylamide gel electrophoresis (SDS-PAGE) (Beyotime, China). The proteins were transferred onto a polyvinylidene fluoride (PVDF) membrane (Millipore, U.S.A.) via wet transfer. The membrane was blocked with 5% non-fat dry milk for 1 h. After blocking, the membrane was incubated overnight at 4°C with primary antibodies: HIF-1α (1:2000, Proteintech, China), HSPA8 (1:2000, Proteintech, China), EIF2AK2 (1:2000, Proteintech, China), and GAPDH (1:10000, Biodragon, China), with GAPDH serving as a loading control. Following washing with PBST (phosphate-buffered saline with Tween-20), the membrane was incubated with Goat Anti-Mouse IgG H&L (1:10000, Biodragon, China) for 2 h. Protein bands were visualized using enhanced chemiluminescence (ECL) reagents (Beyotime, China) for 10 min, and images were captured using an infrared laser imaging system (Odyssey, LI-COR Biosciences, U.S.A.). Relative protein expression levels were quantified using Image-Pro Plus software (Media Cybernetics, U.S.A.).

Statistical analysis

The Mann-Whitney U test was utilized for statistical analysis between the two groups of continuous variables, as they do not adhere to a normal distribution. The Wilcoxon non-parametric test was used to evaluate the significance of the expression differences of the hub gene between the hub gene and the HC group at different time points. For difference analysis and enrichment analysis, the 'Benjamini-Hochberg' method was used to adjust the p value. Significance was determined by the threshold $p < 0.05$.

Result

Differentially expressed autophagy-related genes in IS

To characterize the gene expression changes in IS patients' whole blood, we utilized the GSE16561 dataset and compared it against healthy control whole blood samples. We identified a total of 565 DEGs associated with IS ($p < 0.05$, $|\log_2 FC| > 0.5$). Of these, 308 genes were upregulated, and 257 genes were downregulated (Figure 2(A)). Subsequently, we intersected the DEGs with ARGs to identify DEARGs in the whole blood of IS patients and obtained 13 DEARGs (Figure 2(B)). The upregulated DEARGs included BNIP3L, EIF2AK2, FOS, GABARAPL2, GNAI3, HIF1A, LAMP2, PRKAR1A, RAB33B, and TNFSF10. The downregulated DEARGs were EEF2, HSPA8, and PRKCQ.

To explore the functions of DEG and DEARG in IS, we performed functional enrichment analysis of these genes. We found that DEG in the blood of IS is mainly enriched in pathways related to the immune system in the BP module pathway, such as immune response regulation, immune response activation and other signaling pathways. In the CC module, DEGs are mainly enriched in cytoplasmic vesicle lumen, cell-substrate junction, etc. In the MF module, DEGs are mainly enriched in pattern recognition receptor activity, immune receptor activity, etc (Figure 3(A)). According to the KEGG enrichment analysis of DEGs, they were chiefly enriched in pathways such as primary immunodeficiency, Th1 and Th2 cell differentiation, and Th17 cell differentiation (Figure 3(B)). The expression pattern of immune-related genes in the whole blood of IS patients is shown to be altered by these results.

We further analyzed DEARG-related functions through GO and KEGG enrichment. In the BP, CC, and MF modules enriched in GO, DEARG is mainly enriched in macroautophagy, autophagosome, ubiquitin protein ligase binding, and other functions (Figure 3(C)). KEGG enrichment analysis showed that DEARG was enriched not only in the autophagy pathway but also significantly in immune-related pathways like PD-L1 expression and the PD-1 checkpoint pathway in cancer, as well as Th17 cell differentiation (Figure 3(D)).

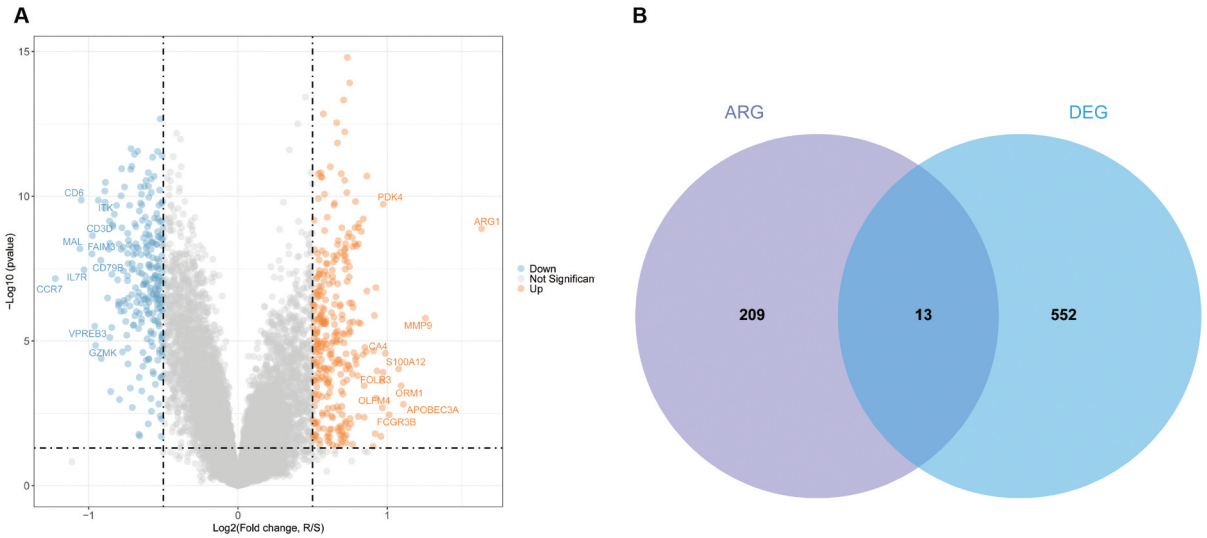

Figure 2. DEARG in IS. (A) DEGs volcano diagram in IS; (B) Venn diagram of DEGs and ARG.

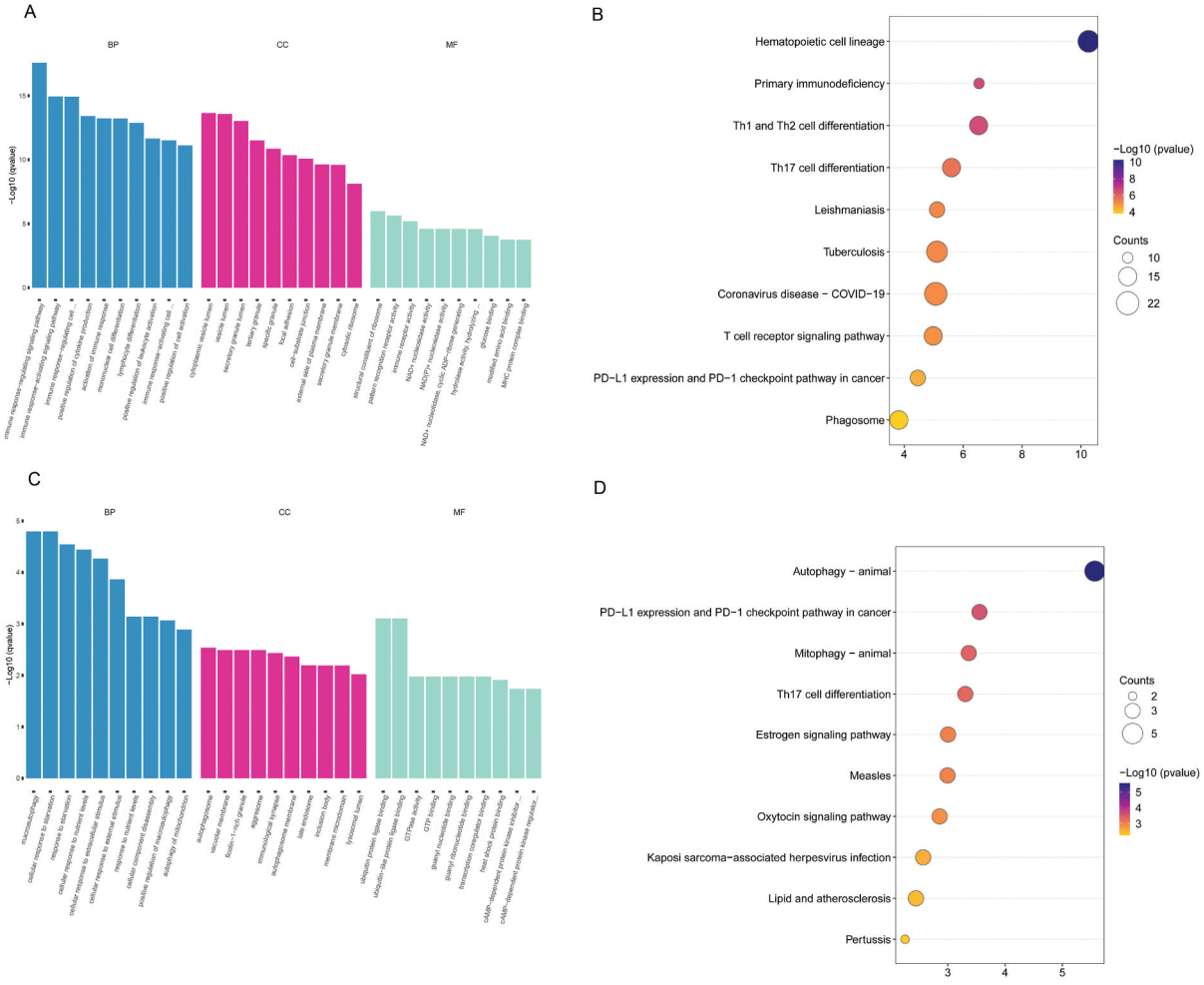

Figure 3. GO and KEGG enrichment analysis of DEGs, DEARGs in IS. (A) Bar Chart of GO Enrichment Analysis for DEGs in IS; (B) Bubble chart of KEGG enrichment analysis for DEGs in IS; (C) Bar chart of GO enrichment analysis for DEARGs in IS; (D) Bubble chart of KEGG enrichment analysis for DEARGs in IS.

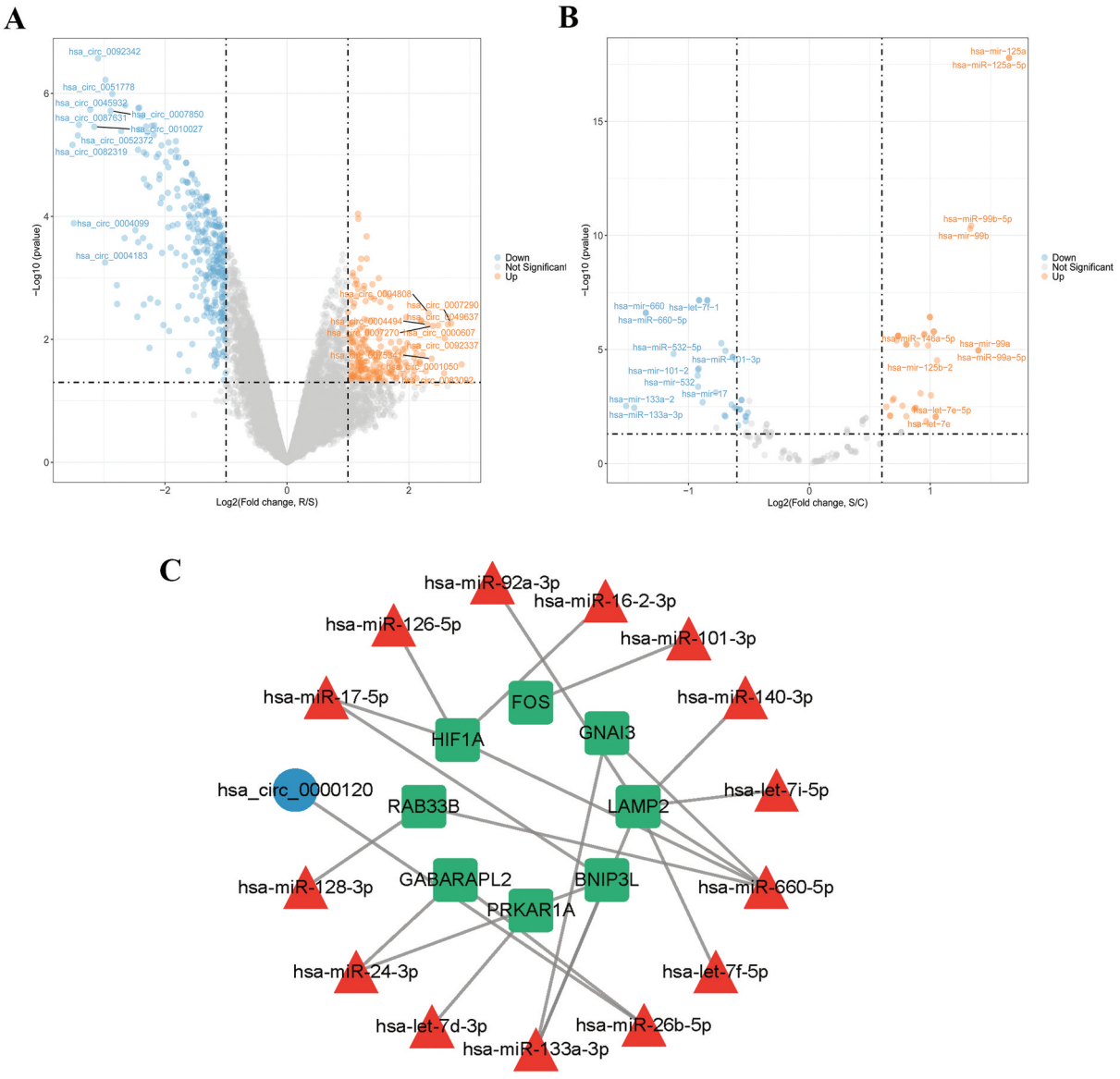

Figure 4. circRNA-miRNA-autophagy-related mRNA network in IS. (A) Volcano diagram of DEcircRNAs in IS; (B) Volcano diagram of DEmiRNAs in IS; (C) ceRNA network constructed based on DEcircRNA-DEmiRNA-DEARG. The green square represents DEARG, the red triangle represents DEmiRNA, and the blue circle represents DEcircRNA.

circRNA-miRNA-autophagy related mRNA network in IS

In order to reveal the regulatory mechanism among DEcircRNAs, DEmiRNAs and DEARGs, we constructed an autophagy-related Competing endogenous RNA (ceRNA) network in IS based on multiple data sets. First, the DEcircRNAs in IS group were screened in the GSE133768 data set. Compared with the HC group, 539 DEcircRNAs were obtained ($p < 0.05$ and $|\log_2 FC| > 1$), of which 218 DEcircRNAs were upregulated and 321 DEcircRNAs were downregulated in IS patients (Figure 4(A)). The GSE199942 data set was used to screen DEmiRNAs in IS. Compared with the HC group, 61 DEmiRNAs were obtained ($p < 0.05$ and $|\log_2 FC| > 0.5$), of which 37 DEmiRNAs were upregulated and 24 DEmiRNAs were downregulated in IS patients (Figure 4(B)). DEcircRNA, DEmiRNA, and DEARG were integrated to construct a ceRNA network, and multiple regulatory relationship pairs were identified, such as hsa-circ-0000120_hsa-miR-26b-5p_GABARAPL2, hsa-miR-24-3p/hsa-miR-17-5p/hsa-miR-13a-3p_BNIP3L, hsa-miR-16–2-3p/hsa-miR-126-5p/hsa-miR-17-5p/hsa-miR-660-5p_HIF1A, hsa-miR-133a-3p/hsa-miR-92a-3p/hsa-miR-140-3p/hsa-let-7f-5p/hsa-let-7i-5p/hsa-miR-660-5p_LAMP2, hsa-miR-133a-3p/hsa-miR-660-5p_GNAI3,

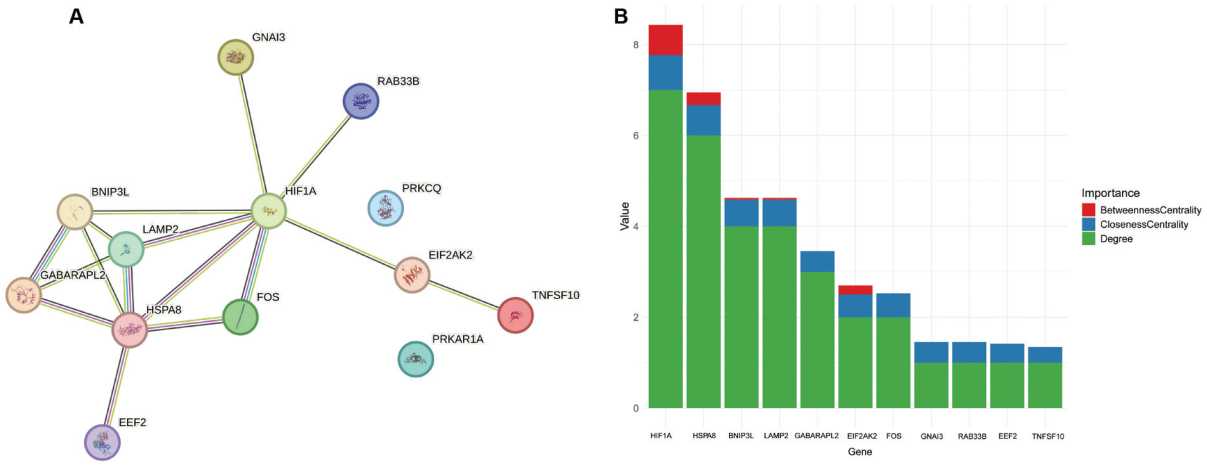

Figure 5. Identification of hub genes in the DEARG network. (A) PPI network of DEARGs. This network visualization illustrates the interconnectedness of DEARGs identified in the study. Each node represents a DEARG, and the edges signify known or predicted interactions between these genes; (B) Stacked bar chart of degree, betweenness centrality, and closeness centrality in the PPI network of DEARGs. This stacked bar chart provides a quantitative assessment of the centrality measures for each node within the DEARG PPI network.

hsa-miR-128-3p/hsa-miR-660-5p_RAB33B, has-let-7d-3p_PRKAR1A, hsa-miR-101-3p_FOS (Figure 4(C)). These ceRNA regulatory relationships suggest the complex regulatory mechanisms of ARGs and may provide more autophagy-related biomarkers.

DEARG hub gene in IS

In our study of IS, we performed an analysis of the PPI network for DEARGs. Our analysis revealed interactions among the DEARGs, with the exception of PRKAR1A and PRKCQ, which did not show interactions with other DEARGs (Figure 5(A)). Hub genes within the DEARG PPI network were determined by considering genes whose degree centrality, betweenness centrality, and closeness centrality were all above the median. This approach led to the identification of five hub genes: HIF1A, HSPA8, BNIP3L, LAMP2, and EIF2AK2 (Figure 5(B)).

Correlation between DEARG hub genes and immune cells

We used CIBERSORT to count immune cells in IS and healthy control blood and perform statistical analysis. The results showed that B cell memory, Macrophages M2, NK cells activated, T cells CD4 memory resting, and T cells CD8 were significantly reduced in the blood of IS patients, while Dendritic cells activated, Monocytes, Neutrophils, Macrophages M0, and T cells CD4 memory activated were significantly increased in the blood of IS patients (Figure 6(A)). We further analyzed the correlation between HIF1A, HSPA8, BNIP3L, LAMP2, EIF2AK2 and differential immune cells in IS patients, and found that all five genes were significantly correlated with Neutrophils, among which HSPA8 was significantly negatively correlated with Neutrophils, while HIF1A, BNIP3L, LAMP2, and EIF2AK2 were significantly positively correlated with Neutrophils. NK cells activated and T cells CD8 were significantly positively correlated with HSPA8, but significantly negatively correlated with LAMP2 (Figure 6(B)). Dendritic cell activation is significantly positively correlated with EIF2AK2, while HSPA8 is significantly negatively correlated with M0 macrophages and activated CD4 memory T cells, and significantly positively correlated with resting CD4 memory T cells. Notably, these genes with the activation levels of immune cells, with p-values < 0.05 and absolute values of correlation coefficients ($|r|$) > 0.3. These results further illustrate that these autophagy-related hub genes may serve as biomarkers of IS.

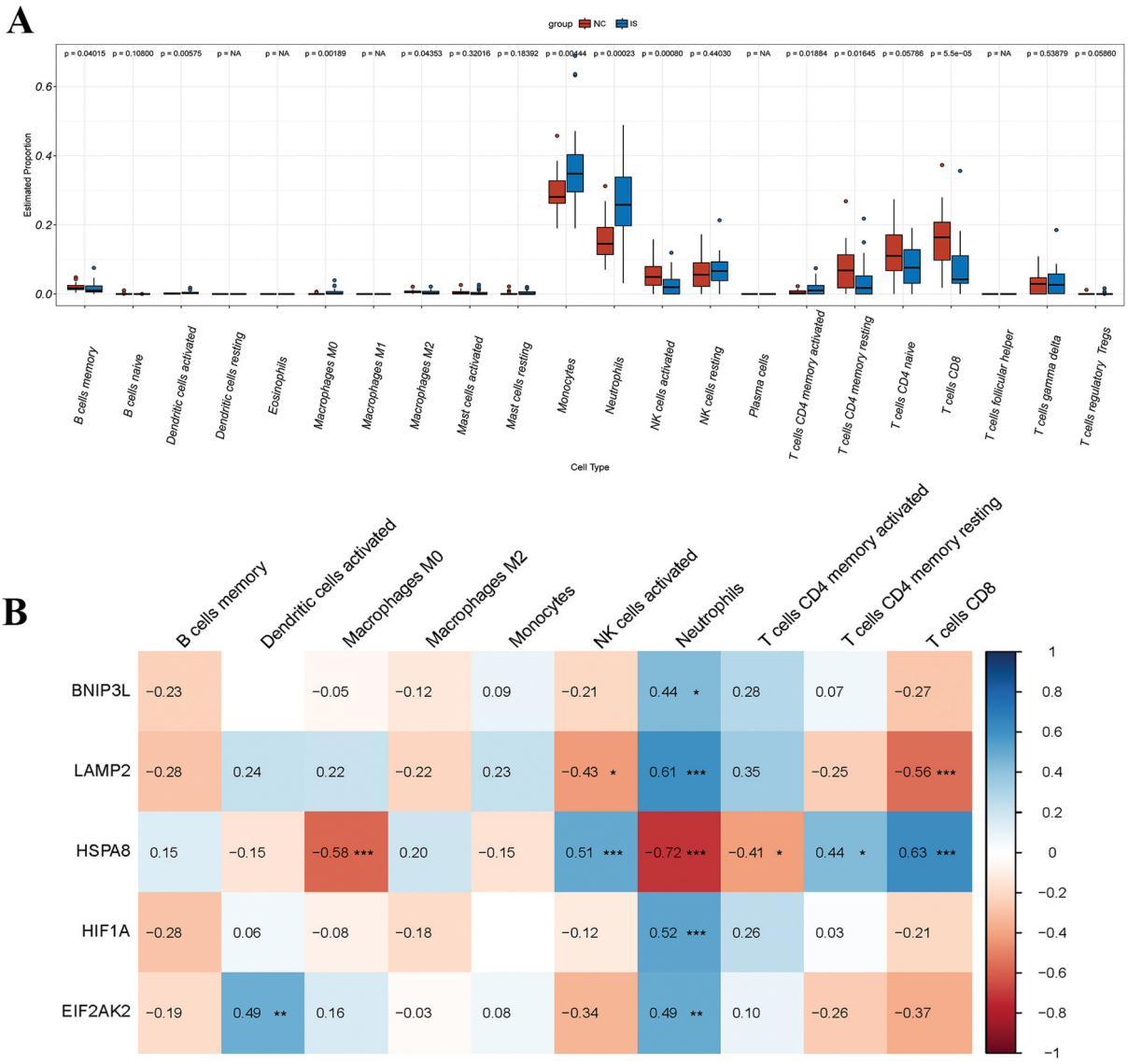

Figure 6. Comprehensive immune landscape of ischemic stroke (IS) patients and the correlation between hub genes and immune cell populations. (A) Box plot illustrating the immune landscape differences between IS patients and Healthy Controls (HC). This box plot visually compares the immune profiles of IS patients with those of HC. Each box represents the distribution of immune cell populations or immune-related metrics; (B) Correlation matrix depicting the relationships between hub gene expression levels and immune cell populations in IS Patients. This matrix presents the pairwise correlations between the expression levels of identified hub genes and various immune cell subsets within the IS patient cohort. Each cell in the matrix contains a correlation coefficient, with asterisks indicating the level of statistical significance: *$p < 0.05$ **$p < 0.01$ ***$p < 0.001$.

Expression verification of hub genes

The data set GSE58294 was utilized to conduct a deeper analysis of the expression patterns of hub genes in IS. The results of the analysis indicated that EIF2AK2, HIF1A, and LAMP2 expression levels were significantly increased compared with the control group at 3, 5, and 24 h after IS. However, the expression of HSPA8 was significantly reduced at 3 and 5 h after IS. Analysis of the GSE58294 dataset showed that although there was a trend toward elevated BNIP3L in the IS group compared to the HC group, there was no significant difference between the IS and HC groups (Figure 7(A)). The expression of HIF1A and EIF2AK2 was significantly elevated at different time points compared to the HC group, and HSPA8 was significantly decreased at 3 and 5 h after the onset of IS compared to the HC group (Figure 7(A)). The expression patterns of the five hub genes were verified by q-PCR in the blood of 20 clinical patients. The results showed that the expression of HSPA8 was significantly

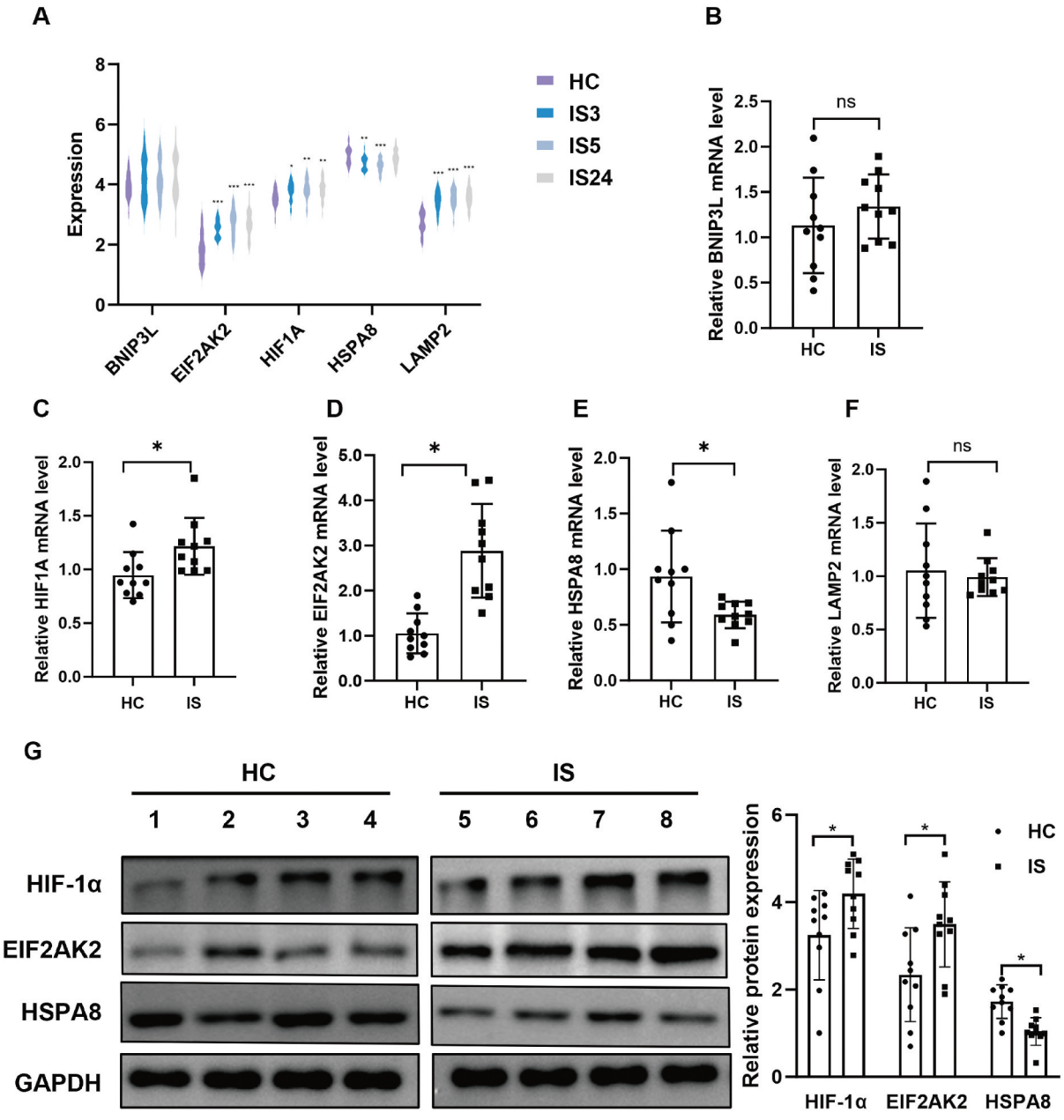

Figure 7. Verification of expression levels of autophagy-related hub genes in is. (A) Temporal expression profile of hub genes following IS onset. This panel illustrates the expression dynamics of identified hub genes at three critical time points after IS occurrence: 3 hours (IS3), 5 hours (IS5), and 24 hours (IS24). (B-F) RT-PCR validation of hub gene mRNA expression in IS and HC Whole Blood. Each subplot compares the expression levels of the respective hub gene between IS patients and HC, with asterisks denoting statistically significant differences ($p < 0.05$); (G) Western blot detection of hub gene protein expression in is and HC blood buffy coat. This panel utilizes western blot analysis to assess the protein expression levels of the hub genes in the blood buffy coat of IS patients compared toHC, * represents $p < 0.05$.

decreased in both IS groups compared to the HC group, whereas the expression of HIF1A and EIF2AK2 was significantly increased in both groups compared to the HC group, and these expression patterns were consistent with the bioinformatic analyses; however, BNIP3L and LAMP2 were not significantly different between IS and HC (Figure 7(B-F)). Finally, we verified the protein levels of HSPA8, HIF1A, and EIF2AK2 in the blood buffy coat of IS patients by Western blot. The protein levels of HIF1A and EIF2AK2 also increased after IS, while the protein level of HSPA8 decreased after IS (Figure 7(G)). These results indicate that HSPA8, HIF1A, and EIF2AK2 May play an important role in the body's response after IS.

Discussion

Using expression profiles from the GEO database, we effectively constructed a circRNA-miRNA-autophagy related mRNA network and identified multiple relationship pairs. Notably, we found significant correlations between the five hub genes identified and immune cell types. Consistently, clinical validation revealed that two autophagy-related genes/proteins were upregulated (HIF1A and EIF2AK2), and one (HSPA8) was downregulated.

Autophagy is widely recognized for its pivotal yet paradoxical role in IS, exhibiting a 'double-edged sword' effect with opposing impacts. Excessive autophagy activation has been shown to exacerbate brain damage. For example, Gong et al. demonstrated that deletion of the autophagy gene Atg7 inhibited neuronal autophagic death and alleviated brain damage in a rat model of cerebral ischemia [25]. Conversely, other studies highlight autophagy's protective effects in stroke. For instance, targeting the key autophagy gene SIRT3 to activate its mediated mitophagy promotes angiogenesis, thereby alleviating cerebral ischemia/reperfusion injury post-stroke [26]. Thus, more studies are required to identify potential biomarkers and investigate the molecular mechanisms of autophagy to support the early diagnosis and treatment of IS.

In our study, PPI analysis of 13 DEARGs yielded five hub genes (HIF1-A, HSPA8, BNIP3L, LAMP2, EIF2AK2). Further validation in clinical samples showed significant upregulation of HIF1A and EIF2AK2 in IS patients, and a significant downregulation of HSPA8. The oxygen content of tissues plays a crucial role in maintaining cellular functions. Short-term hypoxia can trigger molecular pathways in various stem cells, including neural stem cells, to protect them from oxidative damage, while severe or long-term hypoxia affects neural stem cells activity, hinders the normal function and repair ability of the nervous system [27]. As is well known, IS is a disease caused by cerebral ischemia and hypoxia, which means that the occurrence of IS may be closely related to key transcriptional regulators involved in adaptive hypoxia. The HIF1A gene encodes HIF-1α, a key transcriptional factor activated under hypoxic conditions, which is highly sensitive to oxygen concentration and regulates various hypoxia-adaptive genes. Under normoxic conditions, HIF-1α is rapidly degraded by the ubiquitin-proteasome system. However, during hypoxia-ischemia (such as in IS), HIF1A is rapidly activated to adapt to the hypoxic environment, thereby activating numerous biological factors to regulate various biological functions. Specifically, during hypoxia, hydroxylase activity is inhibited, allowing HIF-1α to escape degradation and become activated. It accumulates and enters the cell nucleus, where it forms a complex with HIF-1β to activate downstream target genes. Accumulated HIF-1α, as a transcription factor, enhances the expression of downstream hypoxia-adaptive genes, which may exacerbate blood-brain barrier leakage and inflammatory responses during acute hypoxia [28]. On the other hand, HIF1A can inhibit hypoxia response element-mediated activation of glycolysis-related genes, leading to defects in neuronal energy metabolism compensation and mitochondrial oxidative stress damage [29]. Some studies have suggested that monitoring HIF1A expression levels can estimate the severity of brain hypoxia and injury [30]. However, other studies have reached opposite conclusions, indicating that HIFs alleviate ischemic stress by mediating metabolic reprogramming [31]. This may be related to the subunits of HIF-1, as HIF-1α and HIF-1β may play different roles during IS [31]. Clearly, our results support the former conclusion, as HIF1A expression levels in IS patients are higher than in healthy individuals, playing a certain promotional role in the development of IS. It is worth mentioning that the study of Ewida et al. the changing trend of in HIF1A in stroke patients (including both ischemic and hemorrhagic subtypes) was consistent with our results [32]. Autophagy is crucial for brain cell survival during IR. Appropriate autophagy has neuroprotective effects, while excessive autophagy can lead to neurotoxicity [33]. Evidence suggests that HIF-1α, upon being transported into the cell nucleus under hypoxic conditions, accelerates the activation of BNIP3/BNIP3L, thereby regulating apoptosis and autophagy through control of BNIP3 [34,35]. This indicates that HIF-1α plays a critical role in regulating the autophagy process during brain hypoxia. Furthermore, HIF1A has micrornas targeting autophagy modulators [36], which seems to indirectly verify our results. HIF-1 can induce the expression of hypoxia-sensitive miRNAs at the transcriptional level, while its expression is also regulated by miRNAs, providing a new target for treating hypoxic damage [37].

EIF2AK2 has been reported to participate in cellular autophagy. Wu et al.'s research suggests that EIF2AK2 May be a key gene in activating autophagy during wound healing and promotes wound healing

by upregulating immune cell levels [38]. Notably, under ischemic conditions, eIF2α is phosphorylated and upregulates autophagy-related proteins such as ATG12, leading to autophagy activation, which is considered a unique autophagy control mechanism [39–41]. Inhibition of PKR activity can block the induction of autophagy by reducing the phosphorylation level of eIF2α [42]. Another hypothesis suggests that under hypoxic conditions, eIF2α is phosphorylated to inhibit overall protein synthesis and further mitigate cellular damage through autophagy [43]. Thus, EIF2AK2 May play a more beneficial role during IS. This study found that HIF1A and EIF2AK2 were significantly upregulated within 72 hours of the onset of cerebral infarction, suggesting that hypoxia maintains cellular function and energy homeostasis by activating autophagy. It is worth noting that bioinformatics analysis indicates that EIF2AK2 is also involved in the pathogenesis of various diseases by regulating miRNA expression [44–46]. Furthermore, multiple studies have confirmed that EIF2AK2 is a key participant in the body's immune response [47–49], which is similar to our results. Autophagy has three distinct forms: macroautophagy, microautophagy, and HSPA8 chaperone-mediated autophagy (CMA). The molecular chaperone protein HSPA8 (Hsc70) specifically recognizes the KFERQ-like pentapeptide motif on substrate proteins, forms a ternary complex, and transports it to the lysosomal membrane. Through lysosomal membrane receptors, the substrate is directly transported across the membrane into the lysosomal lumen for degradation [50,51]. HSPA8 is widely involved in IS-related cellular processes and is associated with the infiltration levels of various immune cells [52–54]. Additionally, it is worth noting that evidence suggests that enhancing CMA can alleviate hypoxia-induced pathology in cardiomyocytes, thereby reducing cell death and toxicity [51]. We speculate that HSPA8 May play a similar role during IS. Recent studies have linked tag SNPs rs10892958 and rs1136141 in the HSPA8 gene with increased risk of IS, suggesting that HSPA8 gene polymorphisms may be associated with IS risk [52]. However, there is no literature report on the mechanism of interference with EIF2AK2 and HSPA8 on stroke.

Immune responses plays a pivotal role in the pathological progression of IS and rapidly emerge as a dominant pathological mechanism following disease onset. Upon ischemic brain injury, the immune system initiates inflammatory responses, releasing inflammatory cytokines and mediators to clear necrotic cells and promote neural and vascular regeneration, aiding brain injury repair [17]. After the occurrence of IS, blood inflammatory biomarkers are significantly elevated, such as high-sensitivity C-reactive protein (hsCRP), tumor necrosis factor-alpha (TNF-α), and lipoprotein-associated phospholipase A2 (Lp-PLA2) [55]. Autophagy serves as a crucial regulator of immunity, participating in antimicrobial defense, immune cell function modulation, inflammation regulation, and immune-related diseases [56]. Functional enrichment analysis of DEGs and DEARGs in IS revealed significant enrichment of immune-related pathways, suggesting that autophagy regulation in IS may be related to immunity. Nonetheless, there is limited understanding of how autophagy influences the immune features of IS. To address this gap, we conducted a correlation analysis involving DEARG hub genes and 22 different immune cells. Compared to HC, significant alterations in immune cell types were observed in the peripheral blood of IS patients, indicative of disrupted immune cell homeostasis and an altered immune states. Among the five hub genes, all exhibited significantly correlations with Neutrophils. HIF1A, BNIP3L, LAMP2, and EIF2AK2 showed positive correlations, implying their potential involvement in neutrophil activation and inflammation modulation, conversely, HSPA8 showed a negative correlation, suggesting a possible role in suppressing inflammatory responses. Importantly, these findings do not establish causality, and further functional studies are warranted to elucidate the mechanistic roles and clinical implications of autophagy-immune crosstalk in the pathogenesis and progression of IS.

circRNA and miRNA are essential in controlling mRNA within biological processes including gene expression, cellular development, and disease onset [57,58]. Recent studies indicate that circRNA and miRNA are involved in the pathogenesis of IS through mechanisms like ferroptosis and immune responses [16,17,59]. Our research, along with published literature, demonstrates that HIF1A is crucial for alleviating acute hypoxic damage. Recent findings confirm the key role of RNA interference (RNAi) miRNA in the hypoxic response pathway. miRNA-18a, miRNA-155, miRNA-199a, miRNA-429, and miRNA-433 have been shown to directly interact with HIF1A [37]. This suggests that miRNAs could be novel targets for treating diseases including IS and myocardial infarction, which involve cerebral ischemia. Our bioinformatics analysis identified regulatory pairs such as hsa-miR-16–2-3p/hsa-miR-126-5p/hsa-miR-17-5p/hsa-miR-660-5p-HIF1A. hsa-miR-126, known for its diverse roles in regulating angiogenesis, inflammatory

responses, and metabolism, emerges as a potential target for treating cardiovascular diseases and tumors. hsa-miR-126 can positively regulate HIF1A, thereby inhibiting endothelial cell dysfunction including migration, proliferation, and angiogenesis. HIF1A is a target of miRNA-126's protective function; their therapeutic modulation could benefit the diagnosis and treatment of IS [60]. Under hypoxic conditions, overexpression of hsa-miR-17-5p inhibits autophagy in CAL-27 cells, promoting cell proliferation and migration [61]. These results suggest that these miRNAs may directly or indirectly regulate HIF1A, participating in the pathogenesis of IS. Additionally, bioinformatics analysis predicted multiple circRNA-miRNA-autophagy related mRNA regulatory relationship pairs. These findings offer a basis and guidance for further investigation into how circRNA, miRNA, and autophagy-related mRNA interact in IS.

However, this study still faces several unresolved limitations. Firstly, the expression data comes from multiple datasets, leading to challenges in overcoming heterogeneity across different platforms. Additionally, the sample sizes, particularly for circRNA ($n = 3$) and miRNA ($n = 5$) datasets, are relatively small, which may affect the reliability and generalizability of the analysis. Specifically, a small sample size may lead to insufficient statistical power and an increased risk of false positives/false negatives, directly affecting the accuracy and reproducibility of differentially expressed molecule screening. It may also result in representativeness bias, masking of population heterogeneity, and instability in network construction. However, considering its complementary role in multi-omics integration and its foundation for subsequent circular RNA-miRNA-mRNA ceRNA network prediction, we ultimately included it in the study. Thirdly, the clinical samples used for validation were collected from a single hospital and are limited in number ($n = 10$), which may influence the interpretation and universality of the results. Single-hospital validation maximizes the regional and medical environment concentration of patient baseline characteristics but may also result in an unbalanced distribution of age and stroke severity. We fully recognize the limitations of single-center validation and plan to conduct future studies using larger-scale, multi-center blood samples. Finally, the potential mechanisms of circRNA and miRNA were predicted only through bioinformatics analysis and still require further validation regarding their autophagy regulation in IS. We plan to systematically elucidate the molecular mechanisms of HIF1A, EIF2AK2, and HSPA5 in autophagy regulation and their functional involvement in the pathological process of ischemic stroke through the construction of in *vitro* cell models and in *vivo* animal experimental systems in the future.

Conclusion

In summary, through bioinformatics analysis, we identified key autophagy-related mRNAs in IS. These key mRNAs could be targets for early diagnosis and treatment of IS. Furthermore, we constructed a circRNA-miRNA-autophagy related mRNA network, which may be involved in regulating the onset and progression of IS. Our findings provide new directions for molecular mechanism research, whose clinical applications require further experimental confirmation.

Abbreviations

IS:	ischemic strokes;
MiRNA:	microRNA;
CircRNA:	circular RNA;
mRNA:	messenger RNA;
ceRNA:	Competing endogenous RNA;
GEO:	Gene Expression Omnibus;
PPI:	protein – protein interaction;
qRT-PCR:	quantitative real-time polymerase chain reaction;
ARGs:	autophagy-related genes;
DEGs:	differentially expressed genes;
DEmiRNAs:	differentially expressed miRNAs;
DEcircRNAs:	differentially expressed circRNAs;
GO:	Gene Ontology;
KEGG:	Kyoto Encyclopedia of Genes and Genomes;
BNIP3L:	FBJ murine osteosarcoma viral oncogene homolog;
EIF2AK2:	FBJ murine osteosarcoma viral oncogene homolog,

FOS:	FBJ murine osteosarcoma viral oncogene homolog;
GABARAPL2:	Gamma-aminobutyric acid receptor-associated protein like 2;
GNAI3:	Guanine nucleotide-binding protein-alpha inhibiting 3;
HIF1A:	Hypoxia-inducible factor 1-alpha;
LAMP2:	Ras-related protein
Rab-33BPRKAR1A:	Lysosomal-associated membrane protein 2;
RAB33B:	Ras-related protein Rab-33B;
TNFSF10:	Tumor necrosis factor (ligand) superfamily member 10.
EEF2:	Eukaryotic Elongation Factor 2;
HSPA8:	Heat Shock Protein Family A (Hsp70) Member 8;
PRKCQ:	Protein Kinase C Theta.

Author contributions

YX: Conceptualization, Data Curation, Investigation, Methodology, Validation, Writing – Original Draft. **JD**: Investigation, Formal Analysis. **DZ**: Conceptualization. **MY**: Conceptualization. **GZ**: Conceptualization, Supervision, Project Administration. **ZZ**: Visualization, Resources. **YX**: Investigation, Resources. All authors contributed to Writing – Review & Editing.

Funding

The author(s) reported there is no funding associated with the work featured in this article.

ORCID

Yuyu Xu http://orcid.org/0009-0000-3726-6345

Acknowledgments

In this study, GEO database is used as data source. We appreciate the efforts of the National Center for Biotechnology Information (NCBI) in creating and distributing the GEO database.

Disclosure statement

No potential conflict of interest was reported by the author(s).

Ethics approval and consent to participate

This study complies with the Declaration of Helsinki and Good Clinical Practice guidelines. The research was under the approval of the Ethics Committee of Shengzhou Hospital of Traditional Chinese Medicine (Approval NO: SZZYK-2024–002). The informed consent form was signed by all participants and their families after obtaining their consent.

Data availability statement

The datasets supporting the conclusions of this article are included within the article. The databases analyzed during the current study are available in the GEO database. The accession numbers for the datasets used in this study are GSE16561, GSE 58,294, GSE 199,942 and GLP 21,825. All data generated or analyzed during this study are included in this published article.

References

[1] World Health Organization. *World stroke day 2022*. [cited 2024 Mar 20]; Available from: https://www.who.int/srilanka/news/detail/29-10-2022-world-stroke-day-2022
[2] Feigin VL, Brainin M, Norrving B, et al. World Stroke Organization (WSO): global stroke fact sheet 2022. Int J Stroke. 2022;17(1):18–29. doi: 10.1177/17474930211065917
[3] Feske SK. Ischemic stroke. Am J Med. 2021;134(12):1457–1464. doi: 10.1016/j.amjmed.2021.07.027

[4] Herpich F, Rincon F. Management of acute ischemic stroke. Crit Care Med. 2020;48(11):1654–1663. doi: 10.1097/ccm.0000000000004597
[5] Cui Z, Kuang S, Yang X, et al. Predictive value of the systemic immune inflammation (SII) index for stroke-associated pneumonia. Brain Behav. 2023;13(12):e3302. doi: 10.1002/brb3.3302
[6] Li F, Gao J, Kohls W, et al. Perspectives on benefit of early and prereperfusion hypothermia by pharmacological approach in stroke. Brain Circ. 2022;8(2):69–75. doi: 10.4103/bc.bc_27_22
[7] Uzuner N, Uzuner GT. Risk factors for multiple recurrent ischemic strokes. Brain Circ. 2023;9(1):21–24. doi: 10.4103/bc.bc_73_22
[8] Siracusa C, Vono N, Morano MB, et al. Clinical application of circular RNAs as biomarkers in acute ischemic stroke. J Pers Med. 2023;13(5):839. doi: 10.3390/jpm13050839
[9] Zhang X, Yan H, Yuan Y, et al. Cerebral ischemia-reperfusion-induced autophagy protects against neuronal injury by mitochondrial clearance. Autophagy. 2013;9(9):1321–1333. doi: 10.4161/auto.25132
[10] Mamytov M, Mamytova E, Toktomametova A, et al. Expression of autophagy and apoptosis biomarkers in patients with acute ischemic stroke. Biomedicine. 2022;42(5):988–991. doi: 10.51248/.v42i5.2091
[11] Chen J, Chen G, Xu X, et al. Bibliometric analysis and visualized study of research on autophagy in ischemic stroke. Front Pharmacol. 2023;14:1232114. doi: 10.3389/fphar.2023.1232114
[12] Bushati N, Cohen SM. Microrna functions. Annu Rev Cell Dev Biol. 2007;23(1):175–205. doi: 10.1146/annurev.cellbio.23.090506.123406
[13] Chen L, Wang C, Sun H, et al. The bioinformatics toolbox for circRNA discovery and analysis. Brief bioinform. 2021;22(2):1706–1728. doi: 10.1093/bib/bbaa001
[14] Cheng AM, Byrom MW, Shelton J, et al. Antisense inhibition of human miRNAs and indications for an involvement of miRNA in cell growth and apoptosis. Nucleic Acids Res. 2005;33(4):1290–1297. doi: 10.1093/nar/gki200
[15] Sun S, Li L, Dong L, et al. Circulating mRNA and microRNA profiling analysis in patients with ischemic stroke. Mol Med Rep. 2020;22(2):792–802. doi: 10.3892/mmr.2020.11143
[16] Xie H, Huang Y, Zhan Y. Construction of a novel circRNA-miRNA-ferroptosis related mRNA network in ischemic stroke. Sci Rep. 2023;13(1):15077. doi: 10.1038/s41598-023-41028-1
[17] Wang XZ, Li S, Liu Y, et al. Construction of circrna-mediated immune-related cerna network and identification of circulating circrnas as diagnostic biomarkers in acute ischemic stroke. J Inflamm Res. 2022;15:4087–4104. doi: 10.2147/jir.S368417
[18] Yang Y, Zhang M, Li Z, et al. Identification and cross-validation of autophagy-related genes in cardioembolic stroke. Front Neurol. 2023;14:1097623. doi: 10.3389/fneur.2023.1097623
[19] Tuohy MC, Hillman EMC, Marshall R, et al. The age-dependent immune response to ischemic stroke. Curr Opin neurobiol. 2023;78:102670. doi: 10.1016/j.conb.2022.102670
[20] Wu F, Liu Z, Zhou L, et al. Systemic immune responses after ischemic stroke: from the center to the periphery. Front Immunol. 2022;13:911661. doi: 10.3389/fimmu.2022.911661
[21] Xu S, Lu J, Shao A, et al. Glial cells: role of the immune response in ischemic stroke. Front Immunol. 2020;11:294. doi: 10.3389/fimmu.2020.00294
[22] Gong K, Yang K, Xie T, et al. Identification of circrna-mirna-mRNA regulatory network and its role in cardiac hypertrophy. PLOS ONE. 2023;18(3):e0279638. doi: 10.1371/journal.pone.0279638
[23] Chen JM, Li XL, Yang Y, et al. Competing endogenous RNA network analysis of the molecular mechanisms of ischemic stroke. BMC Genomics. 2023;24(1):67. doi: 10.1186/s12864-023-09163-1
[24] Dong Q, Han Z, Tian L. Identification of serum exosome-derived circrna-mirna-tf-mRNA regulatory network in postmenopausal osteoporosis using bioinformatics analysis and validation in peripheral blood-derived mononuclear cells. Front Endocrinol (Lausanne). 2022;13:899503. doi: 10.3389/fendo.2022.899503
[25] Gong C, Hu C, Gu F, et al. Co-delivery of autophagy inhibitor ATG7 siRNA and docetaxel for breast cancer treatment. J Control Release. 2017;266:272–286. doi: 10.1016/j.jconrel.2017.09.042
[26] Wei J, Xie J, He J, et al. Active fraction of Polyrhachis vicina (Roger) alleviated cerebral ischemia/reperfusion injury by targeting SIRT3-mediated mitophagy and angiogenesis. Phytomedicine. 2023;121:155104. doi: 10.1016/j.phymed.2023.155104
[27] Burtscher J, Mallet RT, Burtscher M, et al. Hypoxia and brain aging: neurodegeneration or neuroprotection? Ageing Res Rev. 2021;68:101343. doi: 10.1016/j.arr.2021.101343
[28] Mohamed MK, Atef AA, Moemen LA, et al. Association study of HIF-1alpha rs11549465 and VEGF rs3025039 genetic variants with diabetic retinopathy in Egyptian patients: crosslinks with angiogenic, inflammatory, and anti-inflammatory markers. J Genet Eng biotechnol. 2022;20(1):122. doi: 10.1186/s43141-022-00401-9
[29] Gladek I, Ferdin J, Horvat S, et al. Hif1a gene polymorphisms and human diseases: graphical review of 97 association studies. Genes Chromosomes Cancer. 2017;56(6):439–452. doi: 10.1002/gcc.22449
[30] Yang F, Gu Y, Yan Y, et al. The association of HIF1A gene polymorphism and its expression with ischemic stroke. Sci Rep. 2025;15(1):14600. doi: 10.1038/s41598-025-99418-6
[31] Madai S, Kilic P, Schmidt RM, et al. Activation of the hypoxia-inducible factor pathway protects against acute ischemic stroke by reprogramming central carbon metabolism. Theranostics. 2024;14(7):2856–2880. doi: 10.7150/thno.88223

[32] Ewida HA, Zayed RK, Darwish HA, et al. Circulating lncrnas hif1a-as2 and linlk-a: role and relation to hypoxia-inducible factor-1α in cerebral stroke patients. Mol neurobiol. 2021;58(9):4564–4574. doi: 10.1007/s12035-021-02440-8
[33] Amin N, Abbasi IN, Wu F, et al. The Janus face of HIF-1alpha in ischemic stroke and the possible associated pathways. Neurochem Int. 2024;177:105747. doi: 10.1016/j.neuint.2024.105747
[34] Tang Z, Zhang Z, Lin Q, et al. Hif-1alpha/bnip3-mediated autophagy contributes to the luteinization of granulosa cells during the formation of corpus luteum. Front Cell Dev Biol. 2020;8:619924. doi: 10.3389/fcell.2020.619924
[35] Chen R, Jiang T, She Y, et al. Effects of cobalt chloride, a hypoxia-mimetic agent, on autophagy and atrophy in skeletal C2C12 myotubes. Biomed Res Int. 2017;2017:7097580. doi: 10.1155/2017/7097580
[36] You L, Wang Z, Li H, et al. The role of STAT3 in autophagy. Autophagy. 2015;11(5):729–739. doi: 10.1080/15548627.2015.1017192
[37] Serocki M, Bartoszewska S, Janaszak-Jasiecka A, et al. Mirnas regulate the hif switch during hypoxia: a novel therapeutic target. Angiogenesis. 2018;21(2):183–202. doi: 10.1007/s10456-018-9600-2
[38] Wu YF, Fang DL, Wei J. Bioinformatics analysis combined with experiments to verify potential autophagy genes in wound healing. Ann Transl Med. 2022;10(12):680. doi: 10.21037/atm-22-2033
[39] Thakor N, Holcik M. Ires-mediated translation of cellular messenger RNA operates in eIF2α-independent manner during stress. Nucleic Acids Res. 2012;40(2):541–552. doi: 10.1093/nar/gkr701
[40] Ahsan A, Liu M, Zheng Y, et al. Natural compounds modulate the autophagy with potential implication of stroke. Acta Pharm sin B. 2021;11(7):1708–1720. doi: 10.1016/j.apsb.2020.10.018
[41] Pan B, Sun J, Liu Z, et al. Longxuetongluo capsule protects against cerebral ischemia/reperfusion injury through endoplasmic reticulum stress and MAPK-mediated mechanisms. J Adv Res. 2021;33:215–225. doi: 10.1016/j.jare.2021.01.016
[42] Shen S, Niso-Santano M, Adjemian S, et al. Cytoplasmic STAT3 represses autophagy by inhibiting PKR activity. Mol Cell. 2012;48(5):667–680. doi: 10.1016/j.molcel.2012.09.013
[43] Wang YC, Li X, Shen Y, et al. Perk (protein kinase RNA-like ER kinase) branch of the unfolded protein response confers neuroprotection in ischemic stroke by suppressing protein synthesis. Stroke. 2020;51(5):1570–1577. doi: 10.1161/strokeaha.120.029071
[44] Wu S, Xue Q, Qin X, et al. The potential regulation of A-to-I RNA editing on genes in Parkinson's disease. Genes (Basel). 2023;14(4):919. doi: 10.3390/genes14040919
[45] Khalko RK, Pandeya A, Saxena S, et al. Hcmv mir-ul70-3p downregulates the rapamycin-induced autophagy by targeting the autophagy-related protein 9a (ATG9A). Int Rev Immunol. 2024;43(4):197–210. doi: 10.1080/08830185.2023.2296488
[46] Zhang Z, Jin H, Zhang X, et al. Bioinformatics and system biology approach to identify the influences among COVID-19, influenza, and HIV on the regulation of gene expression. Front Immunol. 2024;15:1369311. doi: 10.3389/fimmu.2024.1369311
[47] Cottrell KA, Ryu S, Donelick H, et al. Activation of PKR by a short-hairpin RNA. Sci Rep. 2024;14(1):23533. doi: 10.1038/s41598-024-74477-3
[48] Wan W, Qian X, Zhou B, et al. Integrative analysis and validation of necroptosis-related molecular signature for evaluating diagnosis and immune features in rheumatoid arthritis. Int immunopharmacol. 2024;131:111809. doi: 10.1016/j.intimp.2024.111809
[49] Xie JW, Guo YF, Fan SH, et al. Treponema pallidum protein tp47 triggers macrophage inflammatory senescence via pkm2-mediated metabolic reprogramming. Int J Biol macromol. 2024;283(Pt 4):137991. doi: 10.1016/j.ijbiomac.2024.137991
[50] Zhang G, Xiang M, Gu L, et al. The essential role of TTC28 in maintaining chromosomal stability via HSPA8 chaperone-mediated autophagy. Proc Natl Acad Sci U S A. 2024;121(50):e2409447121. doi: 10.1073/pnas.2409447121
[51] Ghosh R, Pattison JS. Chaperone-mediated autophagy regulates hypoxic pathology in cardiomyocytes. Autophagy Rep. 2023;2(1). doi: 10.1080/27694127.2023.2174337
[52] Kobzeva KA, Soldatova MO, Stetskaya TA, et al. Association between hspa8 gene variants and ischemic stroke: a pilot study providing additional evidence for the role of heat shock proteins in disease pathogenesis. Genes (Basel). 2023;14(6):1171. doi: 10.3390/genes14061171
[53] Li G, Cheng Y, Ding S, et al. Identification of key genes associated with oxidative stress in ischemic stroke via bioinformatics integrated analysis. BMC NeuroSci. 2025;26(1):3. doi: 10.1186/s12868-024-00921-9
[54] Zhang X, Xu T, Wang C, et al. Revealing the potential role of hub metabolism-related genes and their correlation with immune cells in acute ischemic stroke. IET Syst Biol. 2024;18(4):129–142. doi: 10.1049/syb2.12095
[55] Dash P, Singh VK, Gautam D, et al. Aspirin resistance and blood biomarkers in predicting ischemic stroke recurrence: an exploratory study. Brain Circ. 2022;8(1):31–37. doi: 10.4103/bc.bc_75_21
[56] Li S, Zhang Y, Shi S, et al. Identification of immune characteristic landscapes related to autophagy in ischemic stroke. Front Cell Dev Biol. 2022;10:1026578. doi: 10.3389/fcell.2022.1026578
[57] Huang W, Wu Y, Qiao M, et al. Circrna-mirna networks in regulating bone disease. J Cell Physiol. 2022;237(2):1225–1244. doi: 10.1002/jcp.30625

[58] Yang Y, Yujiao W, Fang W, et al. The roles of miRNA, lncRNA and circRNA in the development of osteoporosis. Biol Res. 2020;53(1):40. doi: 10.1186/s40659-020-00309-z
[59] Yuan L, Chen W, Xiang J, et al. Advances of circRNA-miRNA-mRNA regulatory network in cerebral ischemia/reperfusion injury. Exp Cell Res. 2022;419(2):113302. doi: 10.1016/j.yexcr.2022.113302
[60] Alique M, Bodega G, Giannarelli C, et al. Microrna-126 regulates hypoxia-inducible factor-1α which inhibited migration, proliferation, and angiogenesis in replicative endothelial senescence. Sci Rep. 2019;9(1):7381. doi: 10.1038/s41598-019-43689-3
[61] Pang F, Liu C, Cui Y, et al. Mir-17-5p promotes proliferation and migration of CAL-27 human tongue squamous cell carcinoma cells involved in autophagy inhibition under hypoxia. Int J Clin Exp Pathol. 2019;12(6):2084–2091.